

Development of Exoplanet database "ExoKyoto" aiming for inter-comparison with different criteria of Habitable zones

Yosuke Yamashiki¹, Takaaki Ito³, Yuji Shimada³, Mariko Inazawa⁴, *Takanori Sasaki², Osamu Nishiura⁴, Shota Notsu², Hiroyuki Ishikawa⁵, Anna Suzuki⁶, Takahito Sakaue⁵, Yuuta Notsu², Naoki Nakamura², Kosuke Namekata⁵, Hiroaki Isobe¹, Kazunari Shibata², Saaya Shimosaki⁷, Shione Fujita⁷

1.Graduate School of Advanced Integrated Studies in Human Survivability Kyoto University, 2.Graduate School of Science, Kyoto University, 3.Faculty of Agriculture, Kyoto University, 4.Faculty of Engineering, Kyoto University, 5.Faculty of Science, Kyoto University, 6.Graduate School of Science, Kyoto Sangyo University, 7.SGH Shiga Prefectural Moriyama High School

An integrated database of confirmed exoplanets, capable in comparing several different definition of Habitable Zone, is developed and launched as "ExoKyoto", for the purpose of better comprehension of those existing celestial entities in different star system. The ExoKyoto core-module is written in C++ with definition of different classes as "ExoPlanet" and "HostStar" objects. The classification of Habitable zone for each host star is based on Kopparapu et al. (2013) as the reference cases, at the same time this database determine Solar Equivalent Astronomical Unit (SEAU) to promote easy comprehension of different star system equivalent to that of Solar System. The database has inter-comparison module with existing exoplanet database as Exoplanet.eu, Open Exoplanet Catalogue, and NASA exoplanet archive, and updating module in order to secure commonly agreed value for each planet. Since most of exoplanets found by Kepler spacetelescope detected only by transit method does not confirmed their mass by radial velocity, a mass estimation module for most of Super-Earth sized planets is included developed based on the Larsen and Geoffrey (2014). Using this mass-assumption module, the portion of Super-Earth sized exoplanets (2-10 Mearth) become dominant (794 among 1988) compared with that of super jovian sized ones (>500 Mearth) (480 among 1988), being comparable to total jovian & super jovian planets (926), in which only 140 of those Super-Earth sized mass has confirmed by radial velocity. Throughout the comparison between habitable criteria by Kopparapu et al. (2013) and ours (SEAU), most of exoplanets orbiting around M type stars have different conditions each other. The potential impact of stellar flares on those exoplanets can be discussed using our database.

For outreach purpose, ExoKyoto possesses interface with GoogleSky for easy comprehension of those celestial bodies among stellar map.

Lauren M. W. and Geoffrey W. M. 2014. The mass-radius relation for 65 exoplanets smaller than 4 earth radii. *The Astrophysical Journal Letters*, 783:L6

Kopparapu R. K. et al. 2013. Habitable Zones Around Main-Sequence Stars: New Estimates. *The Astrophysical Journal*, 765:131

Keywords: Exoplanet, Habitable Zone, SEAU

observation and analysis of exoplanets by using Dipol-2 of T60 telescope at Haleakala mountain

*Haruaki Maeda¹, Takeshi Sakanoi¹, Masato Kagitani¹

1.Planetary Plasma and Atmospheric Research Center, Graduate School of Science, Tohoku University

We have started continuous observation of exoplanets from January 2015 by a method of polarimetry using DIPOL-2 (a double image high precision polarimeter, Piirola et al., 2014) attached to Haleakala T60 telescope. The light scattered or reflected in the planetary atmosphere is linearly polarized. An observer receives the polarized light from the exoplanet as well as non-polarized light from a main star. Thus, periodic variation of linear polarization is observed as the exoplanet orbits around the main star. The polarimetry gives us an information about orbital elements of the exoplanet as well as their atmosphere, even if they do not transit the main stars. Practically, maximum degree of polarization is about an order of 10^{-4} through 10^{-5} for typical hot Jupiter. Because of difficulties of such a high-precision polarimetry, there is only a successful polarimetry of exoplanet (Berdyugina et al., 2008, 2011). One of the primal goal of this study is to establish an observing technique and a analysis method for high-precision polarimetry. To achieve high-precision polarimetry better than 10^{-5} , we need to determine instrumental polarization carefully. First, we analyzed measurements of two high-polarized star (HD204827, HD25443) which enable us to determine reference axis of linear polarization. Then we made analysis of non-polarized standard stars to determine the instrumental polarization. In 2015, we have observed non-polarized standard stars 19 in January, 12 in May, 18 in August and 10 in October, 59 in total. Then, we derived instrumental polarization at accuracy of 10^{-5} , except for the data in January which do not have enough tracking accuracy. We also have several measurement of three exoplanets (tau Boo b, HD189733 b, 55 Cnc e). We would be able to get variation of polarization of exoplanets by subtracting instrumental polarization from the observed polarization. We chose hot Jupiter type exoplanets as observing targets, because they rotate around the main stars by two or three days and we can get polarimetric measurements in the different phase angle within a short time. In this presentation, we will present the recent result of instrumental polarization, method of estimation of the exoplanets' polarization and the recent result from the three exoplanets.

Keywords: exoplanet, polarization, observation, atmosphere, scattering

UV space telescope for exoplanetary systems

*Hiroki Horikoshi¹, Shingo Kameda², Go Murakami³, Masahiro Ikoma⁴, Norio Narita⁵

1.Graduate School of Science, Rikkyo University, 2.School of Science, Rikkyo University,
3.Institute of Space and Astronautical Science, Japan Aerospace Exploration Agency, 4.Department of
Earth and Planetary Science, Graduate School of Science, The University of Tokyo, 5.National
Astronomical Observatory of Japan

Many observations have been carried out for exoplanets since they were first discovered in 1995. To date, the number of detected exoplanets is more than 1900. Some of them are known about their atmospheric composition.

Compared the Earth with the planets which exist in solar system, the Earth has much more oxygen which is produced by photosynthesis. Therefore, detection of oxygen on planets is one of the key factors to characterize exoplanets. In this work, we aim to detect O I emission (130.6 nm) in planet atmospheres by using UV space telescope.

Because planets orbit around its parent star, light of planets whose wavelength is slightly changed with Doppler shift is observed. Therefore, if Doppler shift is large and the parent star's continuum doesn't exist, emissions of planets can be separated from light of its parent star by using high dispersion spectrometer. Because the habitable zones of low-temperature stars are near the parent star, if an Earth-like planet exists in the habitable zone of a low-temperature star, the orbital velocity is fast and the Doppler shift is large. In this work, we assume that the Earth exists in the habitable zones of low temperature star. Then, planetary O I emission can be separated from its parent star. However, because its intensity is very weak, we need to use a large and high efficiency telescope, which exceeds Hubble Space Telescope.

NASA and ESA are planning to launch space telescope dedicated to exoplanets; however, their spectral ranges are limited to the visible and infrared regions. Therefore, we are planning to develop a UV space telescope dedicated to exoplanetary systems. In this presentation, we introduce the study situation and specification of instruments.

Keywords: exoplanet, ultraviolet, space telescope

BepiColombo Euro-Japan Joint mission to Mercury

*Hajime Hayakawa¹, Hironori Maejima¹

1.The Institute of Space and Astronautical Science/Japan Aerospace Exploration Agency

BepiColombo is a ESA-JAXA joint mission to Mercury with the aim to understand the process of planetary formation and evolution in the hottest part of the proto-planetary nebula as well as to understand similarities and differences between the magnetospheres of Mercury and Earth.

The baseline mission consists of two spacecraft, i.e. the Mercury Planetary Orbiter (MPO) and the Mercury Magnetospheric Orbiter (MMO). JAXA is responsible for the development and operation of MMO, while ESA is responsible for the development and operation of MPO as well as the launch, transport, and the insertion of two spacecraft into their dedicated orbits.

MMO is designed as a spin-stabilized spacecraft to be placed in a 600 km x 11400 km polar orbit. The spacecraft will accommodate instruments mostly dedicated to the study of the magnetic field, waves, and particles near Mercury. While MPO is designed as a 3-axis stabilized spacecraft to be placed in a 400km x 1500 km polar orbit. Both spacecraft will be in same orbital plane.

Critical Design Review(CDR) for MMO project is completed in November 2011 while ESA Spacecraft CDR is completed in November 2013. MMO stand alone FM AIV is completed on March 2015. MMO FM was transported to ESA/ESTEC on April. Stand alone activity for MMO was completed in December 2015. MMO is waiting for the stack level (MCS) final AIV. BepiColombo is expected to be launched in 2017. BepiColombo science working team (SWT) meeting, which discusses science related matters, was held once a year and will be held twice a year from this year. In this paper, BepiColombo project as a test case of large collaboration between ESA and JAXA will be reported.

Keywords: Mercury, Planetary Exploration, International Collaboration

JUICE/GALA-J (2): Science objectives of the GAnymede Laser Altimeter (GALA) for the JUICE mission

*Jun Kimura¹, Shunichi Kamata⁵, Koji Matsumoto², Shoko Oshigami², Noriyuki Namiki², Kiyoshi Kuramoto⁵, Sho Sasaki⁸, Keigo Enya⁴, Masanori Kobayashi³, Shingo Kobayashi⁶, Hiroshi Araki², Hiroto Noda², Ko Ishibashi³, Yoshifumi Saito⁴, Hauke Hussmann⁷, Kay Lingenauber⁷

1.Earth-Life Science Institute, Tokyo Institute of Technology, 2.National Astronomical Observatory Japan, 3.Chiba Institute of Technology, 4.ISAS/JAXA, 5.Hokkaido University, 6.National Institute of Radiological Sciences, 7.German Aerospace Center, 8.Osaka University

The Jupiter Icy Moons Explorer (JUICE), led by European Space Agency, has started development toward launch in 2022 (arrival at Jupiter in 2029, and Ganymede orbit insertion in 2032), and we are now developing the GALA instrument onboard JUICE spacecraft collaborating with German Aerospace Center (DLR) and other institutions in Europe. Primary objective of GALA is to acquire the key information for understanding the evolution of icy bodies and to play an essential role in the JUICE's purpose: exploration of deep habitat.

Jovian icy moon Ganymede, which is the largest moon in the Solar System and the primary target of the JUICE, can be said to be one of the typical solid bodies along with terrestrial planets in terms of its size and the intrinsic magnetic field originated from the metallic core. However, current knowledge provided by previous explorations is extremely limited since it comes from only several fly-bys. The JUICE will uncover the whole picture of Ganymede by the first "orbiting" in the history around extra-terrestrial moon. Expected new big picture of the origin and evolution of Ganymede will not only be a key to unveil the origin of diversity among the Solar System bodies, but also contribute to understand exoplanets with a wide diversity.

The GALA will measure a distance between the spacecraft and the surface of icy moons and acquire the topography data (globally for Ganymede, and fly-by region for Europa and Callisto). It will be a first-ever laser altimetry for the icy object. Such information makes surface geologies clear and tremendously improves our understanding of the icy tectonics. By comparing their tectonic styles on the rocky planets/moons, GALA data leads to reconsider the Earth's plate tectonics. In addition, the GALA will confirm a presence/absence of the subsurface ocean by measuring tidal and rotational response, and also the gravitational information reflecting the interior structure will be greatly improved. In addition, strength and waveform of laser pulse reflected from the moon's surface have information about surface reflectance at the laser wavelength and small scale roughness, and therefore we can see degrees of erosion and space weathering without being affected by illumination condition through GALA measurements.

In order to interpret and understand such measurements, accumulated studies for the Earth over the years will be effectively utilized: e.g., the data for surface topography, roughness and albedo will lead to describe the icy tectonics through the knowledge from terrestrial glaciology and experiments on impact and deformation process. The tidal measurements by GALA will also be a window to see its interior based on our knowledge and experiences cultivated through the past geodetic observations, e.g., the SELENE mission for the terrestrial Moon.

Characterization of the icy moons will be achieved not only from the GALA measurements but also synergy of other scientific instruments onboard JUICE spacecraft, for examples, surface images taken by optical camera (JANUS) will confirm the position of GALA laser footprint to complement the GALA "point" data for precise topographic mapping. A radar sounder (RIME) and a radio science experiment (3GM) probe the interior structure, especially interior of the icy crust to figure out an occurrence of tectonic features. A visible and infrared imaging spectrometer (MAJIS), an

ultraviolet imaging spectrograph (UVS) and a sub-millimeter wave instrument (SWI) will acquire a surface and atmosphere compositional data. A magnetometer (J-MAG) monitors moons' inductive response to the Jovian magnetic field and probes the subsurface ocean with the help of a particle environment package (PEP) and a radio and plasma wave investigation (RPWI). The GALA works closely together with these instruments and plays a leading and a supporting role to clarify the whole picture of Ganymede and other icy moons.

JUICE/GALA-J (3): Performance model simulation of Ganymede Laser Altimeter (GALA) for the JUICE mission

*Hiroshi Araki¹, Noriyuki Namiki¹, Hiroto Noda¹, Ko Ishibashi², Keigo Enya³, Masanobu Ozaki³, Takahide Mizuno³, Shin Utsunomiya³, Yoshifumi Saito³, Kazuyuki Touhara³, Shoko Oshigami¹, Shingo Kashima¹, Jun Kimura⁴, Shingo Kobayashi⁵, Masanori Kobayashi², Gregor Steinbruegge⁶, Alexander Stark⁶, Christian Althaus⁶, Simone DelTogno⁶, Kay Lingenauber⁶, Hauke Hussmann⁶

1.National Astronomical Observatory of Japan, 2.Planetary Exploration Research Center, Chiba Institute of Technology, 3.Institute of Space and Astronautical Science, Japan Aerospace Exploration Agency, 4.Earth-Life Science Institute, Tokyo Institute of Technology, 5.National Institute of Radiological Sciences, 6.Deutsches Zentrum für Luft- und Raumfahrt

The laser altimeter GALA (GANymede Laser Altimeter) is one of the payload instrument of JUICE (JUperiter ICy moons Explorer) project led by ESA to be launched in 2022. GALA is developed by the international collaboration by Germany, Japan, Switzerland, and Spanish teams.

In order to clarify the requirement on the interface conditions between modules of GALA, we developed the performance model of GALA based on the model of BELA (Bepi-Colombo Laser Altimeter). The performance model quantifies the link budget, range accuracy, albedo measurement accuracy, and probability of false detection (PFD). In the performance model, background noise from scattered sunlight from the Ganymede surface, surface and bulk dark currents of APD, noise floor of APD-TIA, shot noise, and speckle noise are taken into consideration. Black-body emission from the Ganymede surface is also taken into account while its influence to SNR is negligible compared with other noises. EMI noise shall be included after the evaluation of the verification model.

Scientific requirements on GALA performance is summarized into the following four criteria: [1] For Europa fly-by, PFD is less than 0.2 from an altitude of 1300 km or lower, [2] Under the worst observation condition for albedo and surface slope of GC0500 (Ganymede Circular Orbit whose height is 500km), the accuracy of the ranging is less than 10 m and PFD is less than 0.2. [3] Under the nominal observation condition of GC0500, the accuracy of the ranging is less than 2 m and PFD is less than 0.1. [4] Under the best observation condition of GC0500, the accuracy of the ranging is less than 1 m and PFD is less than 0.1.

Returned laser pulse is converted to analogue signal in Japanese Analogue Electric Module (AEM), then to digital signal and transferred to Swiss Range Finder Module (RFM). RFM applies matched filtering to the digital signal to determine the range as accurately as possible. The signal processing in RFM constrains the performance of AEM, therefore, GALA-J developed its own matched filter simulation aiming to determine the signal-to-noise ratio (SNR). The matched filtering in RFM is a convolution of signal and Gaussian filter whose width in time domain is adjustable. The filtering is thus equivalent to moving average weighted by Gaussian filter in time domain. In this simulation, the length of range gate is 8192 and the sampling frequency is 66.7 MHz which is lower than the current design of ADC of 200 MHz. The band-pass filtering by trans-impedance amplifier of APD (APD-TIA) is taken into account by filtering the return pulse and APD noise by 100 MHz. By changing input SNR and width of the Gaussian filter, the lower bounds of the output SNR that satisfy the system requirements are investigated. The requirements for the input SNR obtained by the investigation are then confirmed well below the analogue SNRs calculated by the performance model.

The return signal is assumed to have a Gaussian form in both spatial and time domain in this performance model, however, the broadening occurs on a reflection by the surface topographic roughness and filtering processes in AEM and RFM. These effects on the results are now investigated and will be shown at the poster presentation.

Keywords: Jupiter, Ganymede, JUICE, GALA, Laser altimeter, Performance model

JUICE/GALA-J (4): Electronics and detector development for Ganymede Laser Altimeter (GALA) for the JUICE mission

*Masanori Kobayashi¹, Osamu Okudaira¹, Ko Ishibashi¹, Masayuki Fujii⁶, Keigo Enya², Noriyuki Namiki³, Hiroshi Araki³, Hiroto Noda³, Shoko Oshigami³, Shingo Kashima³, Masanobu Ozaki², Takahide Mizuno², Shin Utsunomiya², Yoshifumi Saito², Kazuyuki Touhara², Jun Kimura⁴, Shingo Kobayashi⁵, Hauke Hussmann⁷, Kay Lingenauber⁷, Thomas Behnke⁷, Simone DelTogno⁷

1.Planetary Exploration Research Center, Chiba Institute of Technology, 2.Institute of Space and Astronautical Science, Japan Aerospace Exploration Agency, 3.National Astronomical Observatory of Japan, 4.Earth-Life Science Institute, Tokyo Institute of Technology, 6.National Institute of Radiological Sciences, 5.National Institute of Radiological Sciences, 6.FAM Science Co., LTD., 7.Deutsches Zentrum für Luft- und Raumfahrt

Ganymede Laser Altimeter (GALA) is scheduled on board JUICE mission by ESA to be launched in 2022. GALA will be developed and manufactured jointly by teams of Germany, Japan, Switzerland, and Spain. Japanese team is responsible for subunits of a receiver unit out of GALA instrument; a backend optics (BEO), a focal plane assembly (FPA) accommodating an APD sensor module and an analog electronic module (AEM). In our poster presentation, the current development status of APD module and AEM of GALA will be reported.

The APD sensor is mounted on a hybrid IC of the APD module including a trans-impedance amplifier (TIA) for signal readout in a wide band width as 100MHz, a thermo-sensor for measurement of the APD sensor temperature and a thermoelectric (TE) cooler for control of the APD sensor temperature to stabilize the temperature as 25 deg-C or so. The APD sensor has an enhanced quantum efficiency of up to 40% at 1060 nm. APD typically has a large temperature dependency of gain. The APD module is equipped with TE cooler and the TE cooler is capable to control the temperature of APD precisely.

The TIA in the APD module outputs voltage signals corresponding to the input light pulses. The voltage signals are fed into the AEM. The transmitted pulses introduced from LHM are attained not to overshoot by a programmable amplifier in the AEM because the following part of analogue signal processing circuit in AEM is to be tuned for signals returned from the target body which are much smaller than the introduced laser pulses. Signal waveform from the introduced laser pulse to the received return pulse is converted to digital data by analogue-to-digital conversion (ADC) circuit and digitized waveform are transmitted to a range finder module (RFM).

As of writing this abstract, we are preparing radiation test campaign of APD to evaluate and qualify the APD sensor of the module and also building a bread board model of AEM to evaluate development challenges in that.

Keywords: JUICE, GALA, APD, Ganymede, Laser Altimeter

JUICE/GALA-J (5): Radiation analysis for Ganymede Laser Altimeter (GALA) for the JUICE mission

*Shingo Kobayashi¹, Simone DelTogno², Masanori Kobayashi³, Masanobu Ozaki⁴, Keigo Enya⁴, Takahide Mizuno⁴, Makoto Utsunomiya⁴, Yoshifumi Saito⁴, Kazuyuki Touhara⁴, Ko Ishibashi³, Noriyuki Namiki⁵, Hiroshi Araki⁵, Hiroto Noda⁵, Shoko Oshigami⁵, Shingo Kashima⁵, Jun Kimura⁶, Christian Althaus², Kay Lingenauber², Hauke Hussmann²

1.National Institute of Radiological Sciences, 2.Deutsches Zentrum für Luft- und Raumfahrt, 3.Planetary Exploration Research Center, Chiba Institute of Technology, 4.Japan Aerospace Exploration Agency, 5.National Astronomical Observatory of Japan, 6.Earth-Life Science Institute, Tokyo Institute of Technology

The radiation environment around the Jupiter consists of electrons and protons that are trapped by the Jupiter's magnetosphere, solar energetic particles and galactic cosmic-rays. The trapped electrons are the most harmful to devices on the JUICE because the trapped electron flux is the most intense and the its penetrability is relatively higher than the other charged particles. The solar energetic particles are of secondary importance in spite of the lower flux because its energy spectrum is hard and the high energy protons easily penetrate a shield.

The most sensitive device to radiation on the GALA is the avalanche photo diode (APD) to detect the laser pulses returned from the Ganymede's surface. The maximum tolerance, total ionizing dose (TID), is relatively lower than the other devices and is 30 krad. Thus, an adequate shielding is required to reduce the degradation of the performance of the APD. In order to estimate the radiation dose at the APD, a simulation application, GALA-sim and GALA-analy, based on Geant4 [1] and ROOT [2] was developed by GALA Japan to estimate the radiation dose during Jupiter cruising. The application can import for a radiation analysis a three dimensional CAD model which is produced as a result of our structural and strength design of the GALA instrument. It also can estimate the influence of secondary neutron production by nuclear reactions in JUICE in addition to the primary trapped electrons and the solar energetic particles.

The preliminary three dimensional model of the GALA Transceiver Unit (TRU), GAL-TRU-i1.4-Shielding, was developed to analyze the radiation dose during the JUICE mission. The average thickness of mass around the APD in this model is 11.4 g/cm² which corresponds to aluminum which 42 mm thickness. The TRU was irradiated with trapped electrons and solar energetic particles by the GALA-sim based on Geant4 version 9.6.p03 and 10.01.p01 and TIDs at the APD due to trapped electrons and solar energetic particles were estimated. They are 21.2 and 0.72 krad (Figure of safety, FoS=2), respectively, if calculated by Geant4.10.01. The sum of TIDs fell below the maximum tolerance of the APD (30 krad). The radiation dose due to the trapped electrons is 30 times higher than that of solar energetic particles as expected. It is found that the trapped electrons with an energy of 10-40 MeV mainly contributes the TID. No dependency on the versions of Geant4 was observed and both results are consistent each other within 3% difference. The result was also confirmed by the calculation by FASTRAD [3].

The total non-ionizing dose (TNID) which is the energy deposition on a material via non-ionizing processes such as Coulomb scattering, nuclear elastic scattering and nuclear reactions, and results in displacement damage is also estimated based on the theory of non-ionization energy loss by [4] with the help of GRAS [5]. The TNID due to the primary trapped electrons, the primary solar protons and the secondary neutron at the APD is 7.52×10^7 MeV/g (FoS=2) which is equivalent to the 50 MeV proton flux of 1.75×10^{10} cm⁻². The contributions of each particles to TNID were 71%, 24% and 5%, respectively.

In summary, we have developed a simulation code to estimate the radiation damage of the devices in GALA instrument. We found the reasonable solution for the radiation shielding of the APD. The results of calculation are used for the radiation test of the APD at a beam irradiation facility and the improvement of the design of TRU.

[1] S. Agostinelli et al., Nucl. Instr. and Meth. A506 (2003) 250-303.

[2] R. Brun and F. Rademakers, Nucl. Inst. & Meth. A389 (1997) 81-86.

[3] TRAD, <http://www.fastrad.net/>

[4] I. Jun et al., IEEE Trans. Nucl. Sci., 50 (2003) 1924-1928.

[5] G. Santin et al., IEEE Trans. Nucl. Sci. 52 (2005) 2294-2299.

Keywords: Jupiter, Ganymede, JUICE, GALA, Laser altimeter, radiation analysis

JUICE/GALA-J (6): Optical/thermal/structural design for the receiver part of the Ganymede Laser Altimeter (GALA) for the JUICE mission

*Keigo Enya¹, Masanori Kobayashi², Ko Ishibashi², Shingo Kashima³, Shin Utsunomiya¹, Satoru Iwamura⁴, Teruhito Iida⁵, Yoshiaki Matsumoto⁵, Masanori Fujii⁶, Naofumi Fujishiro⁷, Tomoyasu Yamamuro⁸, Masanobu Ozaki¹, Takahide Mizuno¹, Yoshifumi Saito¹, Kazuyuki Touhara¹, Noriyuki Namiki³, Hiroshi Araki³, Hiroto Noda³, Shoko Oshigami³, Jun Kimura⁹, Christian Althaus¹⁰, Simone DelTogno¹⁰, Kay Lingenauber¹⁰, Hauke Hussmann¹⁰

1.Institute of Space and Astronautical Science, Japan Aerospace Exploration Agency, 2.CIT, 3.NAJO, 4.MRJ, 5.PLANET, 6.FAM Science, 7.Astro-Opt, 8.OptCraft, 9.Earth-Life Science Institute, Tokyo Institute of Technology, 10.DLR

We present Optical/Structural/thermal design for the receiver part of the Ganymede Laser Altimeter (GALA) for the Jupiter Icy Moon Explorer (JUICE) mission. JUICE is a mission of ESA to be launched in 2022, and GALA is one of the payloads of JUICE. For the laser altimetry, GALA emits and receives laser pulses at about 500 km altitude above Ganymede. Wavelength, energy, and repetition frequency of the laser plus are 1064 nm, 17 mJ, and 30 Hz, respectively. Reflected beam from the Ganymede surface is received by the receiver telescope with 25 cm diameter aperture, re-focused by the BEO including a narrow band-pass filter, and then detected by the APD detector. In the international collaboration, GALA-Japan will develop the Backend Optics (BEO), the Focal Plane assembly (FPA) including an avalanche photo-diode (APD) detector, and the Analog Electronics module (AEM) in the receiver chain.

Thermal environment of GALA is unique: The Receiver telescope and some parts are cooled to intermediately cryogenic temperature by radiation to the cold surface of Ganymede and deep space while the APD detector has to be kept at 25 degree in its operation time. Many parts of GALA are warmed by self-heating. Furthermore, GALA repeats observation time of 16 hours and data downlink time of 8 (power of observation part is off) hours. So the thermal environment is dynamic. On the other hand, GALA have to keep stability of optical performance, especially absolute agreement of the optical axis of the emitter and the receiver and to the spacecraft coordinate system. Radiation shield also has to be mandatory. Considering these conditions, we are carrying out design of optics, structure and thermal design for the BEO, FPA, and AEM. The current baseline design, the BEO is simply consisting of a collimator lens, a narrow band-pass filter, a focusing lens supported without adhesive. The material used for the structural material of both BEO and FPA must have small thermal expansion and good radiation shielding. Iterative studies of thermal analysis of whole GALA and the optical/thermal/structural design is ongoing.

Keywords: JUICE, GALA, optical/thermal/structural design

Non-destructive material identification of volatile particles using translational motions induced by magnetic field gradient

*Keiji Hisayoshi^{1,2}, Wakana Yamaguchi¹, Chiaki Uyeda¹

1.Dept. of Earth and Space Science, School of Science, Osaka University, 2.Kasugaoka High School

Recently, we developed a new method of magnetization measurement method, in which translation induced by the magnetic field gradient was used, and proposed a material identification based on this method. Due to the field-induced energy, the solid particles which were released in a diffused area (in a condition that effect of gravity and viscous drag are negligible), causes translational motion by a practical field intensity of the permanent magnet. Because this motion derives from a magnetic volume force, the motion of the particle is independent to the mass. The material possesses the intrinsic susceptibility per unit mass. Therefore, the material of individual particles can be estimated by comparing the measured susceptibility with a list of published values. In the present study, we apply the above method to identify volatile solid grains of H₂O and CO₂.

The translational motion is observed by the chamber-type drop box. The system was realized by introducing small Nd-Fe-B plates. The setup for observing the motion was attached inside a rectangular volume of 35x30x20 cm of a drop box. The setup was enclosed in a vacuum chamber; the sample motion was observable from the outside of the Pyrex wall of the chamber, using a high-speed video camera that had time resolutions of 0.033 s. The pressure of the medium inside the chamber was P =100 Pa. Duration of μ G was about 0.5sec with residual gravity of 0.01G.

Previously, identification of particles using magnetic field was limited on materials with spontaneous magnetization. However, it's possible to expand the method to general solid particles. Provided that the motion of particle is observable, it's possible to measure the susceptibility of the sample no matter how small the particle may be. In the field of the organic chemistry and the biochemistry, the method to separate a mixture of organic molecules has been established by introducing the technique of chromatography. The proposed principle of material identification can be applied in an apparatus developed for a mission to examine the surface of the icy satellites.

Reference

- [1] K. Hisayoshi, S. Kanou and C. Uyeda : Phys.:Conf. Ser., 156 (2009) 012021.
- [2] C. Uyeda, K. Hisayoshi, and S. Kanou : Jpn. Phys. Soc. Jpn. 79 (2010) 064709.

Keywords: non-destruction distinction, translational motion , magnetic field gradient force, microgravity, volatile particle

Electromagnetic induction in icy moons of Jupiter - A review and its future perspective

*Hiroaki TOH¹, Taka'aki Katsura²

1.Data Analysis Center for Geomagnetism and Space Magnetism, Graduate School of Science, Kyoto University, 2.Department of Earth and Planetary Sciences, Graduate School of Science, Kyoto University

Internal oceans of icy moons of gas giants of our solar system are among recent hot topics in planetary sciences. Newly discovered evidence for hydrothermal vents in the liquid ocean of Enceladus (Hsu et al., 2015) is still fresh in our memory. Presence of the internal oceans is one of the necessary conditions for extra terrestrial life, although interaction of liquid water with the lithosphere of the icy moon in concern via, say, the hydrothermal activity, is also indispensable. It, therefore, worth revisiting the problem of internal oceans of Jupiter's Galilean satellites with icy surfaces at this time of coming successive Jovian probe missions such as Juno (Bagenal et al., 2014), JUICE (ESA, 2014) and so on.

The latter three of the four Galilean satellites, Io, Europa, Ganymede and Callisto, are covered with ice, while intense volcanic activity is ongoing on the Io's surface due to the immense tidal force of Jupiter. Those volcanic ejecta become a dense source of plasmas of Io origin, which results in Io's footprints of Jupiter's auroras (e.g., Bonfond et al., 2013). It is noteworthy that the former three of the Galilean satellites have those footprints, while Callisto alone lacks in them implying a very thin plasma environment around that moon as it is the farthest to Jupiter without any significant source of plasmas from Callisto itself. This means that Callisto is least subject to the plasma effect in terms of electromagnetic induction.

Another feature of Callisto that is worth noting is its orbital state. While the former three revolutions are in the state of Laplace Orbital Resonance (Murray and Dermott, 1999), Callisto alone is out of it. This may cause a significant difference in tidal force which each moon feels. Tidal dissipation is one of the important factors (Chen et al., 2014) when we consider the heat source that maintains the internal oceans of the icy moons, if any.

In this study, we reanalyzed the vector magnetic field data at the time of Galileo Probe flybys around Callisto. Assuming a time-varying uniform external magnetic field (Khurana, 1997; Khurana and Schwarzl, 2005) with a direction almost parallel to the direction of Jupiter looking from Callisto, we calculated the induced dipole field generated by concentric spherical shells. As a result, a conductive shell with a similar conductivity of seawater on the Earth was found when the depth to it was constrained by an assumed phase diagram of water inside Callisto, which coincides with previous studies (Khurana et al., 1998; Zimmer et al., 2000).

However, if the internal structure of Callisto is significantly different from those of Europa and Ganymede in the sense that Callisto has experienced immature differentiation unlike rest of the two, Callisto may provide a better platform for extra terrestrial life by an increased chance for liquid water-lithosphere interaction. In this presentation, the obtained electrical structure will be further examined comparatively with that of Europa known to date. Comparison with that of Ganymede may be subject to another research because of the moon's peculiar intrinsic core field.

Keywords: Icy moons, Jupiter, Electromagnetic induction

Stability of liquid methane on Titan's surface

*Shuya Tan¹, Sho Sasaki²

1.Department of Earth and Planetary Science, Graduate School of Science, The University of Tokyo,

2.Department of Earth and Space science, Graduate School of Science, Osaka University

Titan has liquid methane on the surface due to surface conditions affected by the temperature profile of its thick nitrogen atmosphere. The purpose of this study is to discuss the stability of the surface environment, by estimating relationships between liquid methane on the surface and parameters which affect characteristic of the atmosphere. The typical parameters are the solar flux, the gravitational acceleration and so on.

Strictly speaking, present state of body like Titan depends on the evolution from its formation. But there are different scenarios for the formation of icy satellites, and moreover, the evolution is modified by external factors such as impacts and tidal heating. Here, we conduct parameter changes on the basis of the present Titan's condition.

We use an analytic radiative-convective model for plate-parallel atmosphere (Robinson et al., 2012). On convective region, we consider the condensation of methane.

In Titan's atmosphere, radiation is affected by absorption of thermal infrared by gas molecules and absorption of visible light by photolysis organic haze, which mainly exists in its stratosphere. The visible absorption by haze causes cooling the surface. We relate the mole fraction of methane to infrared absorption coefficient (Nakajima et al., 1992). The strength of visible absorption is probably changed by methane concentration in stratosphere and haze optical property and so on. In the present study, for simplicity, we hypothesize the simple cases, the strength of haze absorption is constant or expressed by simple function.

On this model, about liquid methane on the surface, the solar flux has lower limit caused by methane condensation. And if greenhouse effect is stronger than cooling by haze, the solar flux can have upper limit. Nitrogen partial pressure on the surface only affects the latter, and the gravitational acceleration affects both.

When the strength of visible absorption by haze is constant, the solar flux has the upper and lower limits regardless of nitrogen pressure on the surface and gravitational acceleration. The present solar flux matches the lower limit when nitrogen partial pressure is 1.06×10^6 Pa or the gravitational acceleration is 0.15 m/s^2 .

A study on surface roughness in thermo-physical modeling of asteroid for the estimation of thermal inertia

*Jun Takita¹, Hiroki Senshu², Satoshi Tanaka³

1.Graduate School of Science, Tokyo University, 2.Chiba Institute of Technology/PERC, 3.JAXA/ISAS

This study reports preliminary results of our study about the effect of rough surface on thermal inertia from thermal phase delay using thermo physical model (TPM). In the thermal modeling of asteroid, information on the surface topography and surface roughness is indispensable for thermophysical estimation, which is especially important to deduce thermal inertia of an asteroid. This is one of the preparations for the thermo-physical observations of asteroid Ryugu using the thermal infrared imager in Hayabusa2 mission.

For numerical approach using TPM, we produced rough surface models by deforming a spherical surface mesh. We considered the effect of surface roughness on surface temperature as a function that changes only the effective emissivity of the planetary surface, following the works of Davidsson et al. (2009) and Leyrat et al. (2011).

We fitted the surface temperatures that were generated by the rough surface models to determine whether the thermal phase delay can still be retrieved under rough surface topographies. We picked only the surface temperatures on the equatorial zone. Quadratic least-square fitting is applied to the data to deduce thermal phase delay.

We evaluated uncertainties in the estimation of the phase delay based on a series of data generated in the diurnal motion. As a result, we found that the feasibility of thermal inertia from the diurnal phase delay depended greatly on the observational geometry in terms of solar illumination over the asteroid surfaces. The thermal phase delay could be determined without being strongly affected by local topography under low solar phase angles. Considering the errors of phase shift, the uncertainty of thermal inertia will be greater than 50% if the rough scale is greater than 9.6° (RMS surface slope angle) from the case of low solar phase angle.

Keywords: asteroid, thermal inertia, surface roughness

Relationship between formation age and the degree of degradation of the lunar craters

Fumiki Muto¹, *Tomokatsu Morota¹, Junichi Haruyama²

1. Graduate School of Environmental Studies, Nagoya University, 2. Japan Aerospace Exploration Agency

Impacts of micro projectiles erode the lunar surface. Unraveling the time-scale for topographic degradation on the lunar surface is fundamental for understanding processes of the migration of regolith and the bombardment history and developing new dating method for the lunar surface. In this study, I performed crater morphologic analysis based on a topographic diffusion model to reveal the relationship between formation age and the degree of degradation for lunar craters and to evaluate the topographic diffusivity on the lunar surface. Digital Terrain Model (DTM) derived by Kaguya/Terrain Camera was used to investigate the crater shapes and the optical maturity parameter (OMAT), which characterizes the immaturity of lunar soils, was used as an indicator of the formation age for craters. The shapes of craters with fresh ejecta show that crater depth is affected by the local subsurface structure, while there is no difference of the slope of inner wall among fresh craters. Therefore, I evaluated the degree of degradation using the slope of inner wall. I found that there is a negative correlation between the degree of degradation and OMAT. Using the relationship the topographic diffusivity was estimated to be 13-31 m²/Myr.

Keywords: crater, crater degradation, impact, Moon

Statistical analyses of bright ray craters on Ganymede: implications from Galileo and Voyager images

*Luyuan Xu¹, Hideaki Miyamoto¹, Naoyuki Hirata²

1.The University Museum, The University of Tokyo, 2.Kobe University

Ray craters are impact craters surrounded by radial rays or ejecta patterns (both bright and dark) and prominent on Ganymede, the biggest satellite of Jupiter. Bright ray craters are recognized to be the youngest features on Ganymede [1], and represent the most recent impact cratering [2]. Also, being susceptible to destruction by various processes [1-3], bright ray craters may inform on the most recent geologic processes on Ganymede.

Passey and Shoemaker [4] identified 84 bright ray craters $D > 30$ km and obtained several preliminary results and conclusions using the image data of Voyager. However, since Voyager 1 and 2 only have sufficient resolution (better than 2 km/pixel) images limiting to the subjovian and antijovian surroundings [4, 5], the analysis of Galileo images could fill in this gap. Also, the revised global geologic map [5] and advanced cratering impact model [2] make a more accurate distribution and a more comprehensive understanding of bright ray craters of Ganymede possible.

In this study, we used the raw images of both Voyager and Galileo images (825 Voyager images and 314 Galileo images) to identify ray craters. Since the crater rays are sensitive to solar illuminations [2] and the coverage limitation of images, we only measured the ray craters at high sun conditions and in the latitudinal range 70°N - 70°S [5]. Also considering the identifiable sizes of ray craters are highly dependent on spatial resolution of images, we initially examined the influence of image resolution on the density distribution of ray craters.

Ultimately, our work resulted in a revised density distribution of bright ray craters corresponding to spatial resolution, latitude, angular apex distance, and different terrain types, finding that the crater density of bright ray craters on Bright Terrain of Ganymede is at least $\sim 4x$ from apex (the center of the leading hemisphere) to antapex (the center of the trailing hemisphere), and the bright rays are likely to be erased at a higher rate with increasing latitudes. Based on our results, we reconsidered the possible reasons for cratering asymmetry on Ganymede [2], and confirmed the influence of latitude-related factors, which might include thermal-driven sublimation [6] and plasma-induced sputtering [7].

References

- [1] Shoemaker E. M. et al. (1982) *Satellites of Jupiter*: 435-520.
- [2] Zahnle K. et al. (2001) *Icarus*, 153, 111-129.
- [3] Schenk P. M. and McKinnon W. B. (1991) *Icarus*, 89, 318-346.
- [4] Passey Q. R. and Shoemaker E. M. (1982) *Satellites of Jupiter*: 379-434.
- [5] Patterson G. W. et al. (2010) *Icarus*, 207, 845-867.
- [6] Squyres S. W. (1980) *Icarus*, 44, 502-510.
- [7] Khurana K. K. (2007) *Icarus*, 191, 193-202.

Keywords: Ganymede, bright ray craters, Galileo images

The discrimination experiment of meteorites using LIBS for the Martian Moons Explorer mission

*Misa Horiuchi¹, Kazuo Shibasaki¹, Yuichiro Cho¹, Shingo Kameda¹, Ko Ishibashi², Koji Wada², Takashi Mikouchi³, Tomoki Nakamura⁴, Seiji Sugita³

1.Rikkyo University, 2.Planetary Exploration Research Center, Chiba Institute of Technology, 3.The University of Tokyo, 4.Tohoku University

Phobos and Deimos are the two satellites of Mars. It is suggested that they originated either through asteroid capture or giant impact [1]. The Japan Aerospace Exploration Agency (JAXA) is planning to launch the Martian Moons Explorer (MMX) in 2022 that aims to return samples from Phobos. It is hoped that these samples will reveal the origin of Phobos and, thereby, will constrain the theory of Solar System formation. The sampling site will be selected based on Phobos' entire reflection spectra to return optimum samples containing intrinsic materials to Phobos. However, the reflection spectra may not provide sufficient information on the composition of Phobos because of space weathering. In addition, the composition of Phobos's surface in particle scale has unknown and isn't known until the samples are returned to the Earth. Therefore, we focused on in-situ measurement of elemental composition, which isn't affected by space weathering. We proposed mounting a laser-induced breakdown spectroscopy (LIBS) on the MMX lander for measuring the elemental composition of the Phobos's surface.

We conducted LIBS experiment to evaluate the feasibility of LIBS measurement on Phobos. We investigated the capability of distinguishing carbonaceous chondrite from Martian meteorites by LIBS, which provides a clue to knowing whether the surface of Phobos is composed of asteroid-like or Martian-like materials. Our experimental system simulated an actual setup for Phobos exploration. We used a small laser with an output of about 12 mJ/pulse and a wavelength of 1534 nm. The wavelength range of the spectrometer was 195 nm to 1128 nm. The distances between the lens to converge the laser beam and the sample, and between the condensing lens of the spectrometer and the sample were both 1.5 m. The effective diameter of the light collection optical system was 20 mm. The samples were placed in a vacuum chamber. We verified the feasibility of LIBS measurement including signal-to-noise ratio under such realistic conditions. The samples were Allende (a carbonaceous chondrite), NWA1068 (a Martian meteorite), and Zagami (a Martian meteorite). The sample was irradiated 150 times on each measurement point with 10 Hz. The exposure time of the spectrometer was 1 s. We measured 16 points per a sample to obtain the bulk composition of the meteorites. The emission spectra of the major elements, Fe, Ca, Al, Mg, Si, and Ti, were detected in the average spectra of 16 measurement points. By subtracting the spectra of the Martian meteorites from that of the carbonaceous chondrite, we found that the intensity of the emission lines of Fe and Mg, which are abundant in the Allende meteorite, exhibit positive values. In contrast, the intensity of the emission lines of Al and Ca, which are abundant in the NWA1068 and the Zagami meteorites, exhibit negative values. Those results show that LIBS can distinguish between asteroid-like and Martian-like materials.

Since the MMX lander can stay on the surface of Phobos for only about 1 hour, we evaluated whether LIBS can conduct the same measurement as our experiment in such a short time. It was assumed that the focus adjustment and image acquisition takes 10 s, and moving from one measurement point to another takes 20 s. The laser irradiation frequency is 2 Hz to save the electric power consumption. Then, it takes 28 minutes to conduct the same data acquisition as our experiment (i.e., measuring 16 points with 150-times laser irradiation per point). This indicates that LIBS can obtain sufficient data within the operation time of the lander. Our results suggest that LIBS can reveal

whether Phobos is similar to asteroids or Mars.

Reference

[1] Fraeman, A. A., et al. (2012), *J. Geophys. Res.*, 117, E00J15.

Keywords: the Martian Moons exploration project, LIBS, in-situ measurement

A new paradigm to solve "the missing link of "Moon and Earth"" is "Multi-Impact Hypothesis", it explains both Origin of the "Moon formation and the Earth's plate tectonics" and Formation of Mercury

*Akira Taneko¹

1. SEED SCIENCE Lab.

In the scientific method to explore the origin of the previous solar system where life, including human beings occur, deductive method, and a creative subjunctive in addition to induction. It means to discover the truth in the induction method, an observation or experiment of Earth evolution. There was nothing other than the Earth observation until now as the way. Hypothesized, the hypothesis is believed as the conclusion is often the more that can explain the current situation.

Now, in the Abduction creative reasoning, is the idea of correctness is increased if be said in reverse. It is a perfect way to explore the origins and mysteries, but If you do not have thought a breakthrough hypothesis, have no sense at all.

The "Multi-Impact Hypothesis," to give the hypothesis with the following "Linking the moon and the earth of the Missing Link," a unified reasoning of (A) and (B).

(A) Differentiated protoplanetary CERRA of Mars size formed in the asteroid belt position of the solar system, by the perturbation of the most recent of Jupiter (giant mass), orbit is flattened to Jupiter near point side.

(B) Immediately before the CERRA to Jupiter collision, ruptured at a tension of Jupiter and the sun, the mantle piece collide intersects the Earth orbit.

by Abduction

(1) Moon of origin: collision mantle piece to Earth (12.4km / s, 36.5 degrees), and formed in the orbit radius $60 \cdot R_e$ position

* (2) Pacific Rim arc-shaped archipelago marginal origin: In the Pacific Ocean position collision at the time of moon formation, Depression marginal sea forming in all directions

* (3) By a large amount of mantle deficient moon formation collision, Van Allen belt of Brazil of core eccentricity (about 10%) was reduced.

* (4) CERRA it takes about 5-6 million years until the track flat torn in Jupiter perturbation, had already differentiated cooling.

* (5) Multiple of mantle piece collide to Earth by peeling off the mantle, 70% of the sea surface of the earth -5km was formed by isostasy.

* (6) Origin of plate tectonics PT, minimization of the eccentric and the moment of inertia caused by the collision as the driving force.

* (7) Origin of plate boundary, Crust peeling due to the mantle piece collision and crack formation

* (8) Origin of arc-shaped archipelago and Marginal basin plate: Mantle deficit by collision and plate concave formed by isostasy

* (9) The origin of the start of subduction convex plate: When the concave plate and the convex plate each other press by the driving force, cause the convex crawl under concave.

(10) Fragments at break of CERRA is the origin of the asteroid belt. Understood in the distribution of long radius (kinetic energy)

(11) The meteorite, but differentiated stony, stony-iron and iron meteorites are mixed, it can be understood with the fragments of CERRA.

(12) There are several fragments of CERRA, large species extinction repeated happened with sequentially collision.

(13) Core and part of the mantle of CERRA, the mass is large energy such as distribution, It became

a low orbital energy Mercury with law of equipartition of energy.

(14)The fragments of CERRA that has collided to Jupiter, was the origin of the Great Red Spot.

(15) Why Pluto is a stony? Jupiter and Saturn is a gas planet! I suggested. "Swing by the Serra fragments became Pluto with Jupiter"

(16)The inclination 23.5 degrees earth's axis was achieved with collision of the high latitude! Kimberlite pipe formation to the Russian Mirny mine position, By the collision of the Drake Passage , It gave a moment that the inclination of the earth's axis is changed.

(17) the inclination of the rotation axis is also changed the direction of the driving force, it can be steep bend also the description of the Emperor seamount chain.

(Description of the sudden change in the thermal convection the drive theory seems to be impossible)

Keywords: the missing link of "Moon and Earth", Origin of the "Moon formation ", Origin of the "Platet ectonics", Abduction, Formation of Mercury, Titius Bode law

8. チチウス・ボーデの法則の 再検討 (1) 2015 10-14

問題点, 8-1. 本仮説での証明方法 種子彰 2015

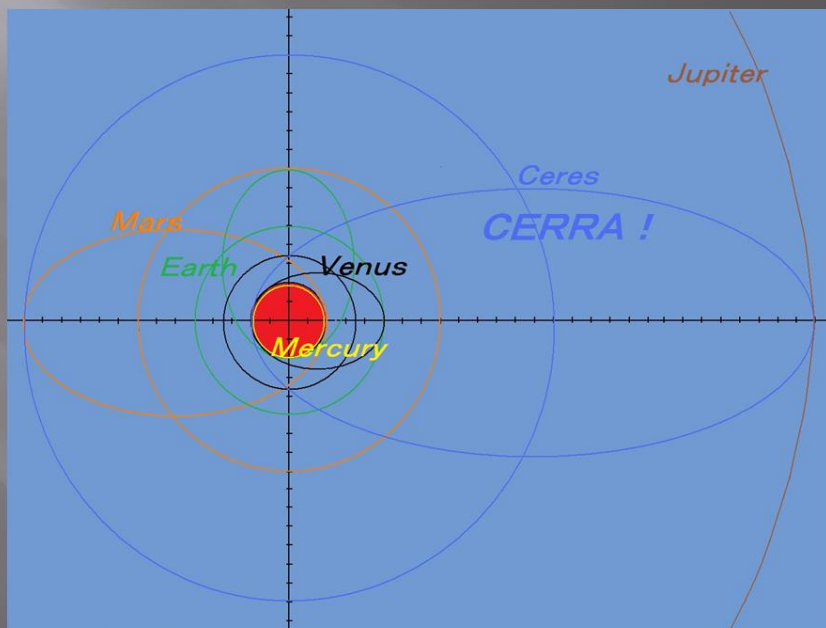
◆水星 $n = -\infty$ この理由が説明できない. ⇒ 禁制帯とマルチインパクト仮説.

◆小惑星帯 $n = 3$ の欠番理由が説明できない. ⇒ CERRAの潮汐関断裂.

◆海王星 $n = 7$ で
の不一致と、冥王星
の一致の理由が説
明できない. ⇒ CE
RRA断裂片のフラ
イバイと海王星衝突

8-1. <証明>

- 禁制帯、フィード
バックゾーンでの合体
- 微惑星楕円軌道
近点での衝突合
体による軌道縮退
- CERRAの潮汐
断裂片⇒水星に.
- 断裂片木星スイ
ングバイ⇒冥王星



Experimental simulations on impact-induced dehydration of porous surfaces

*Jinshi Sai¹, Ryo Ogawa², Akiko Nakamura², Yusuke Seto², Kazunori Ogawa²

1.Graduate school of science, Tokyo University, 2.Graduate school of science, Kobe University

It is now generally believed that accretion of planetesimal formed planets and collision with small-bodies evolved them. Impact-induced dehydration of impactors influenced the composition of primitive planetary atmosphere and the supply of water to planets. So it is required to understand impact-induced dehydration of planetary bodies in terms of the origin of water-planets. Lots of works about small bodies to reveal the origin of the solar system and planets have been performed including sample return missions from primitive bodies. Asteroid exploration Hayabusa2 will return samples of a C-type asteroid Ryugu which possibly has hydrated minerals. Understanding impact-induced dehydration is of importance in order to discuss the influence of dehydration of the returned samples.

A lot of experimental works related with impact-induced dehydration have been performed and most of the experiments are shock recovery experiments. In this method, the samples were capsuled in sealed metal containers and impacted by projectiles indirectly. This method derived impact-induced water loss as a function of shock pressure, but didn't simulate real surface of planetary bodies very well because of the container. The relation between sample porosity and water loss has also been studied but is not fully understood. In order to discuss dehydration of asteroids due to impacts, it is necessary to reveal the relationship between dehydration efficiency and porosity in detail. In this study, we performed shock dehydration experiments without sealed containers to simulate natural impacts on the surface of planetary bodies. In addition, we used gypsum targets with different porosities and examined the relationship between porosity and shock-induced water loss. We set the sample in a cylindrical stainless container and shot a disk-shaped metal, stainless-steel or copper, projectile directly onto the surface. Targets were set inside a vacuum chamber under 0.1atm condition. We measured the velocity of projectile using a high-speed video camera. The shock pressure was calculated by impedance matching method. The post-shocked samples were recovered from the surface of the projectile. We analyzed the recovered samples by XRD and examined if dehydration occurred. After that, we measured the impact-induced water loss (wt%) by thermogravimetric analysis (TGA) and compared the results with those of XRD. Impact-induced dehydration was observed in this study. We found that the results of XRD and TGA were consistent. We did not find any strong relationship between porosity and water loss in this work.

Keywords: impact-induced dehydration, porosity

Effect of secondary collision and target texture on three-dimensional shape distribution

*Tokiyuki Kadokawa¹, Akira Tsuchiyama¹, Tatsuhiro Michikami², Sunao Hasegawa³, Tsukasa Nakano⁴, Kentaro Uesugi⁵

1.Department of Earth and Planetary Sciences, Graduate School of Science, Kyoto University, 2.Kinki University, 3.ISAS/JAXA, 4.AIST, 5.JASRI/SPring-8

3D shape distributions of regolith particles returned from the asteroid Itokawa by the Hayabusa mission and the moon by the Apollo and Luna missions have been measured [1,2]. Such 3D shape distributions reflect conditions of regolith particle formation and it is important to compare with those of fragments in laboratory impact experiments to discuss impact processes on the surfaces of Itokawa and the moon.

It has been proposed based on a laboratory experiment that the 3D shapes of impact fragments have characteristic distribution; the average axial ratios of the longest, intermediate and shortest lengths of fragments, $a : b : c$, is $2:\sqrt{2}:1$. Although the ratios of individual fragments were widely distributed [3]. As this result was obtained only in a catastrophic disruption condition, Michikami et al. [4] carried out impact experiments under wide range of impact conditions from cratering to catastrophic disruption and found that the average three axial ratios is not $2:\sqrt{2}:1$ when the impact energy density is low (cratering conditions). However, the size of fragments examined (>4 mm) is bigger than that of Itokawa and Luna regolith particles (20-300 μm). So, we measured the axial ratios of fragments obtained from the same experiments [4] with similar size to the regolith particles, and found that (1) the size distribution depends on the fragment size, (2) the average axial ratios are almost constant around $2:\sqrt{2}:1$ irrespective of the impact energy density and (3) the distribution cannot be distinguished from that of Itokawa particles [5]. However, effects of secondary collision and target texture have not been evaluated.

In this study, additional experiments were made in order to elucidate the effect of secondary collision and target texture. Impact experiments were carried out with a two-stage light-gas gun at JAXA. We used basalt, dunite, ordinary chondrite (L4/5) and lead glass as targets and spherical nylon (7.14 mm in diameter) or alumina (1.00 mm) as projectiles. The impact velocity ranged from 1.60 to 7.0 km/s. Two types of impact fragments (30-600 μm) were examined; one is fragments collected in aerogel, which were not suffered by secondary disruption, and the other is fragments collected from the surfaces of impact absorbers. The three axial lengths were measured using X-ray microtomography in SPring-8, and their 3D shape distributions were compared with each other and with those of Itokawa and Lunar regolith particles using Kolmogorov-Smirnov test.

It was found from the experiments that the 3D shape distributions and the average axial ratios of fragments collected from aerogel cannot be distinguished from those from the impact absorber surfaces. This indicates the fragments measured by Kadokawa et al. [5] were not influenced by secondary collision or secondary collision little affected the 3D shapes. It was also found that the 3D shape distributions of the experiments using basalt targets cannot be distinguished from those using dunite and ordinary chondrite targets, while they can be clearly distinguished from those using homogeneous lead glass target, which is largely different from basalt in textures. This suggests that experiments using basalt targets can simulate impact processes on the asteroids. The present results indicate that the results of Kadokawa et al. [5] is applicable to Itokawa and Luna particles; Itokawa particles can be formed by collisional destruction, but we cannot estimate their impact conditions from the 3D shape distribution while the values of the average axial ratios of Luna particles, which is closer to unity, suggests that they were affected by gardening in the regolith layer.

[1] Tsuchiyama et al. (2011) *Science*, 333,1125-1128. [2] Sakurama et al. (2015) JpGU Abstract PPS23-P10. [3] Fujiwara et al. (1978) *Nature*, 272, 602-603. [4] Michikami et al. (2015) *Icarus*, 264, 316-330. [5] Kadokawa et al. (2015) JSPS Abstract 04-05.

Effects of oblique impacts on catastrophic disruption of rocky bodies simulated by quartz glass

Yuu-saku Yoshida¹, *Masahiko Arakawa¹, Minami Yasui¹, Kazunori Ogawa¹, Chisato Okamoto¹

1. Graduate School of Science, Kobe University

Planetary collisional process is one of the most important physical processes in the solar system, especially for the planetary formation process in the solar nebulae. Because of the importance of the physical process and the implications for the origin of asteroids and other small bodies, impact disruption experiments have been conducted for several decades, and rocky materials such as basalt and glass etc. were used for these impact experiments. Then, the impact strength defined by the specific energy (Q) necessary for the catastrophic disruption was obtained for these rocky materials, and most of the impact experiments were conducted by head-on collisions, so that the impact strength was usually applicable only for the head-on collision. However, collisions among planetary bodies are well known to be not only head-on collision but also oblique collision, and actually the impact angle of 45 degrees is the most probable impact angle in the solar system. Therefore, it is necessary to study the impact strength for the oblique impact and to clarify the effect of oblique impact on the collisional disruption of rocky bodies.

In this study, we conducted the impact experiments of quartz glass at the impact angle from 90 (head-on collision) to 0 (glancing impact) degrees, and studied the effect of oblique impacts on the degree of disruption and the ejection velocity of the ejecta fragments. We used quartz glass spheres with the size of 5cm and 8cm for the target, and a polycarbonate spherical projectile with the size of 4.75mm was launched at the impact velocity from 2 to 6km/s. The oblique impact was made at 15 to 90 degrees at 4.3km/s under the vacuum condition of 20Pa. After the impact, all the impact fragments were recovered to measure each weight in order to construct the size distribution of these fragments.

We found that the largest fragment mass was almost constant at the impact angle from 90 to 60 degrees, and it suddenly decreased from 60 to 45 degrees for the 5cm target, and then gradually increased up to 15 degrees: the largest fragment mass at 45 degrees was one order of magnitude larger than that obtained from the impact between 90 and 60 degrees. Although the impact strength could be strongly affected by the impact angle at the high obliquity smaller than 45 degrees, the modified specific energy (Q_c) defined by the normal component of the impact velocity on the impact surface was an appropriate parameter to scale the impact angle on the degree of the impact disruption, then the impact strength (Q^*) could be refined by using this modified specific energy, Q_c : The obtained impact strength defined by Q_c including the oblique impacts is 1110 J/kg for the quartz glass. We also found a very unique feature on the quartz glass during the disruption, that is, the severe disruption and high velocity ejecta was discovered at the antipodal region. The mass of disrupted fragments originated from the antipodal region was almost same as that was originated from the cratered region near the impact site. This might be caused by the severe concentration of the shock wave at the antipodal region and it would be reflected on the free surface with the perfectly spherical shape of the quartz glass. But, further research would be necessary to understand this unique features discovered at the antipode.

Keywords: catastrophic disruption, oblique impact, impact strength

Shock induced vitrification, defect generation, and change in cathodoluminescence of quartz: possibility as a new shock barometer

*Yu Chang¹, Masahiro KAYAMA², Eiichi Tajika³, Yasuhito Sekine¹, Toshimori Sekine⁴, Hirotsugu Nishido⁵, Takamichi Kobayashi⁶

1.Department of Earth and Planetary Science, Graduate School of Science, The University of Tokyo, 2.Planetology, Kobe Univ., 3.Complexity Sci. & Eng., Univ. of Tokyo, 4.Earth & Planetary Sci., Hiroshima Univ., 5.Research Institute of Natural Science, Okayama Univ. of Science., 6.National Institute for Material Science (NIMS)

Impact cratering is a ubiquitous process on both terrestrial planets and small bodies in the solar system. Researches for impact craters on the Earth provide a valuable opportunity to constrain planetary-scale impact event. In particular, reconstruction of shock pressure recorded in the shock-metamorphosed minerals leads to a clue to understand a partition of the impact energy and cratering mechanism on Earth.

Quartz, which is one of the most abundant and widely distributed rock-forming mineral on the Earth's crust, has been widely used to evaluate shock pressure on the impactite. However, the conventional shock estimations based on the mineralogical features of quartz, such as PDFs, are no more than a qualitative approach, hence it is required for more detailed evaluation of shock pressure to develop new advanced method using quartz.

Recently, we found the drastic change in cathodoluminescence (CL) features of quartz due to shock metamorphism [1]. The blue emission intensity (450-460 nm) of shocked quartz increases drastically with the experimentally induced pressure and reaches up to 100 times as large as that of the starting materials. On the other hand, CL intensity around 630 nm changes less than 3 times in spite of the pressure increase. Therefore, the relationship between shock pressure and blue CL intensity could be used as a new shock barometer. The mechanism for the increase in the blue CL intensity, however, still remains unclear because of a lack of information on structural defect in shocked quartz. In this study, Raman spectroscopy and EBSD analysis were conducted for the experimentally shock-induced quartz to clarify the structural change and generation of misorientations with the pressure. Consequently, we elucidated the CL mechanism of shocked quartz by comparison with the obtained Raman and EBSD data.

Raman spectra of the shocked quartz show a weakening of the main peak at $\sim 464\text{ cm}^{-1}$ with pressure increase. At 30 GPa, the new peak at $\sim 495\text{ cm}^{-1}$ appears, indicating the generation of shock-densified silica glass [2]. EBSD mapping revealed that shocked quartz undergo high pressure ($\sim 20\text{ GPa}$) has high-density domains with boundary misorientation dominated by 60° , suggesting the development of Dauphiné twinning. However, for the quartz undergo pressure over 30 GPa, EBSD diffraction pattern was unrecognised because of low crystallinity. Therefore, the blue CL emission is closely related to Dauphiné twin, but this phenomenon is limited to the pressure lower than 30 GPa. On the other hand, the destruction of crystal structure and generation of high-density silica glass are consistent with the continuous increase in CL intensity of blue emission with pressure increase. These facts indicate a spectral change depending on the extent of vitrification. The relationship between CL intensity and the possibility as a new shock barometer will be also discussed.

[1] Chang et al., (2015) JpGU Meeting, PPS22-19.

[2] Okuno et al., (1999) PCM, 26, 304-311.

Keywords: shock metamorphism, shocked quartz, cathodoluminescence, micro-Raman spectroscopy, EBSD

Radiation mechanism of the Chelyabinsk superbolide

*Masahisa Yanagisawa¹

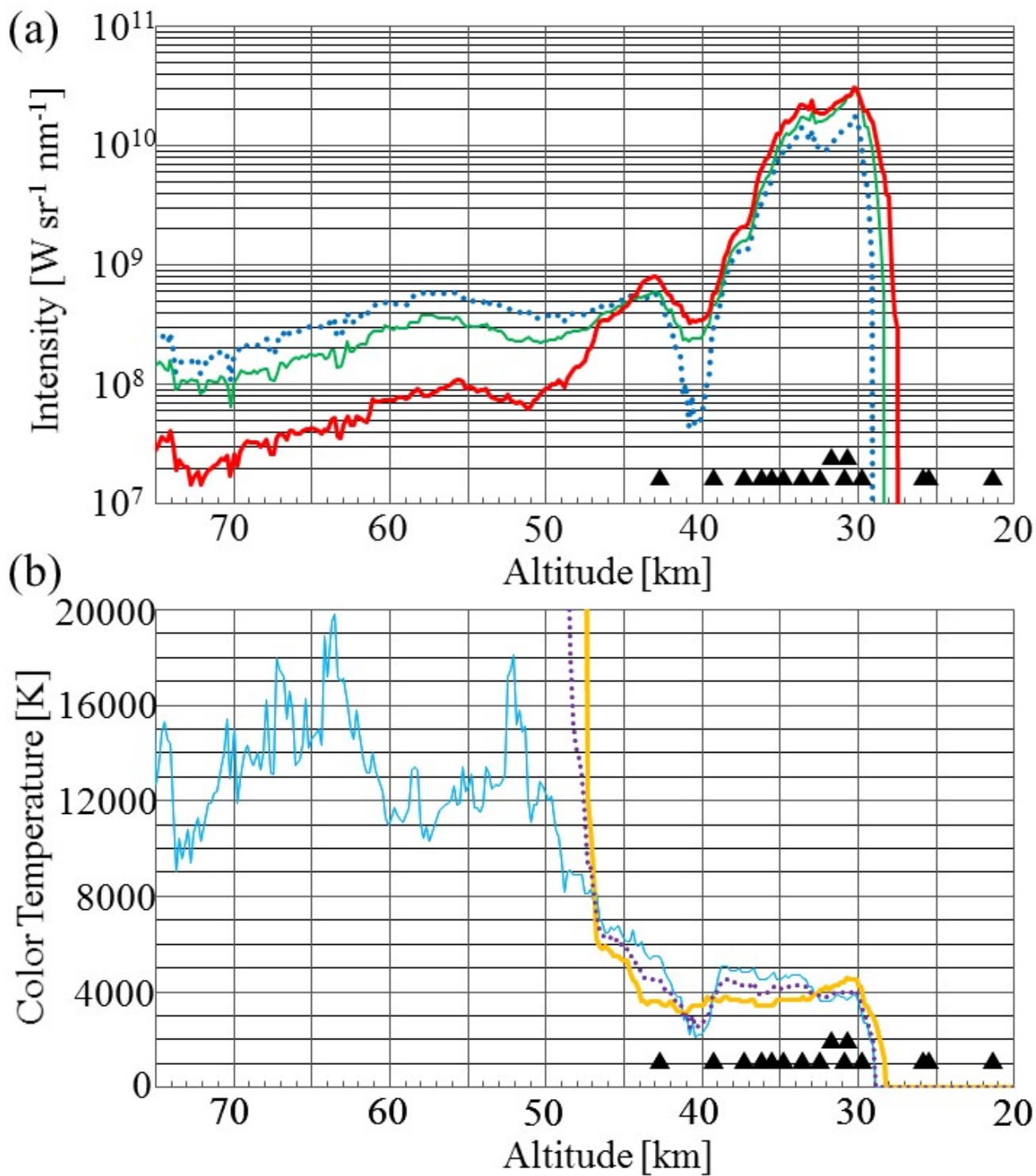
1. The University of Electro-Communications

On Feb. 15, 2013, a meteoroid with a size of about 19 m plunged into the terrestrial atmosphere at 19 km s^{-1} and burst at an altitude of about 30 km over the city of Chelyabinsk, Russia. Here we present light curves for the bolide in the red, green, and blue color bands, derived from an analysis of a video that was recorded by a dashboard camera and released on the Internet (Fig. 1). Our results demonstrate that the bolide was blue-green in color, which is inconsistent with the Planck spectrum before the meteor began to fragment. Fragmentation triggered a flare-up of the bolide and 90% of its radiation energy at optical wavelengths was released within a period of about 2 s after that. During the same period, the brightness ratios among the three bands became consistent with 4000 K blackbody radiation. Based on the peak luminosity, a surface area of several square kilometers would be required for a 4000 K blackbody. It is considered that the radiation source of the bolide was an elongated cloud of vapor and debris produced through severe fragmentation of the meteor.

Reference: M. Yanagisawa, Radiative characteristics of the Chelyabinsk superbolide, *Planetary and Space Science.*, 118C, 79-89, 2015.

Figure 1. (a) Bandpass photometric intensities for the Chelyabinsk bolide plotted as functions of the bolide altitude. The thick, thin, and dotted lines respectively show the intensities in the R, G, and B bands. The black triangles indicate the altitudes at which meteor fragmentation occurred, with the upper two triangles corresponding to severe fragmentation events. (b) Color temperatures for the bolide as functions of altitude. The thick, thin, and dotted lines show the temperatures based on the R/G, G/B, and R/B intensity ratios, respectively. The error is expected to be about $\pm 400 \text{ K}$.

Keywords: Chelyabinsk, bolide, fireball, meteor, meteoroid, hazard



Capture of small bodies by a giant planet

*Arika Higuchi¹, Shigeru Ida²

1.Tokyo Institute of Technology, 2.Earth-Life Science Institute, Tokyo Institute of Technology

We have investigated the dependence of the prograde/retrograde temporary capture of asteroids by a planet on their original heliocentric semimajor axes through analytical arguments and numerical orbital integrations in order to discuss the origins of irregular satellites of giant planets. We found that capture is mostly retrograde for the asteroids near the planetary orbit and is prograde for those from further orbits. An analytical investigation reveals the intrinsic dynamics of these dependences and gives boundary semimajor axes for the change in prograde/retrograde capture. The numerical calculations support the idea of deriving the analytical formulae and confirm their dependence. Our numerical results show that the capture probability is much higher for bodies from the inner region than for outer ones. These results imply that retrograde irregular satellites of Jupiter are most likely to be captured bodies from the nearby orbits of Jupiter that may have the same origin as Trojan asteroids, while prograde irregular satellites originate from far inner regions such as the main-belt asteroid region.

Keywords: irregular satellites, small bodies

Capture of planetesimals by gas drag

*Ryo Suetsugu¹, Keiji Ohtsuki¹

1. Graduate School of Science, Kobe University

Regular satellites of the giant planets in the Solar system are moving on nearly circular and coplanar orbits, thus they are thought to be formed in circumplanetary gas disks. Solid materials in the circumplanetary disk that formed satellites are supplied from the protoplanetary disk. Canup & Wards (2002) assumed that the major building blocks of regular satellites are meter-sized or smaller bodies that are brought to the disk with the gas inflow from the protoplanetary disk. On the other hand, supply of solid bodies to circumplanetary disks has been recently studied in detail using orbital integration (Fujita et al. 2013, Tanigawa et al. 2014). These works showed that bodies that are sufficiently large to be decoupled from the gas flow can contribute to the formation of regular satellites. Influence of captured solid bodies on satellite system formation would vary depending on the timing of capture. When planetesimals are captured by gas drag from the circumplanetary disk in the midst of accretion of regular satellites, part of captured planetesimals would contribute to the growth of satellites, while the rest spirals into the central planet. However, the circumplanetary disk dissipates at some point due to either gap formation in the protoplanetary disk or global dispersal of the protoplanetary disk. Planetesimals captured by such a waning circumplanetary gas disk would survive in the disk for a long period of time, and may become irregular satellites after the dispersal of the disk.

However, capture of planetesimals by weak gas drag from waning circumplanetary disks has not been examined in detail. Cuk & Burns (2004) examined capture of irregular satellites by waning disks in the late stage of planet formation, and discussed the origin of a cluster of prograde irregular satellites of Jupiter. Assuming that the cluster members are collisional fragments derived from a single body, they integrated orbits of the cluster progenitor backward in time until it escaped from the planet's Hill sphere, taking account of weak gas drag from the circumjovian disk. They found that some planetesimals captured into prograde orbits about Jupiter likely experienced a period of temporary capture before permanent capture. However, Cuk & Burns (2004) mainly focused on the capture of prograde irregular satellites and did not examine capture and orbital evolution of retrograde irregular satellites.

In the present work, we examine capture of planetesimals in waning circumplanetary gas disks using three-body orbital integration. In addition to the process of capture, we also examine subsequent orbital evolution of captured planetesimals. We find that some of captured planetesimals can survive in the circumplanetary disk for a long period of time under such weak gas drag. Captured planetesimals have semi-major axes smaller than about one third of the planet's Hill radius. Distributions of their eccentricities and inclinations after disk dispersal depend on the strength of gas drag and the timescale of disk dispersal, and initially strong gas drag and quick disk dispersal facilitates capture and survival of planetesimals. However, in such a case, final orbital eccentricities and inclinations of captured bodies remain rather large. Although our results suggest that some of the present irregular satellites of gas giant planets with small semi-major axes would have been captured by gas drag, other mechanisms are required to fully explain their current orbital characteristics.

Also, gas drag capture was proposed as the origin of the Martian satellites, but has not been examined in detail. Thus, we also examine capture of planetesimals by gas drag from a spherically symmetric atmosphere.

Keywords: Planet, Satellite, Planetesimal

Possibility of Planetesimal Formation in Disk Formation Stage

*Kenji Homma¹, Taishi Nakamoto¹

1.Department of Earth and Planetary Sciences, Tokyo Institute of Technology

Planets are formed from planetesimals, so it is important to reveal planetesimal formation processes to elucidate the origin of our solar system and extrasolar planetary systems. It is thought that planetesimals are formed from micrometer-sized grains called "dust", which are present in the protoplanetary disk. They collide each other, coagulate, and grow to form planetesimals. However, there are some obstacles in this process. One of the most serious obstacles is the "radial drift barrier": macroscopic aggregates experience the head wind from the disk gas, lose their angular momentum with respect to the central star, and drift toward the star.

On the other hand, it is suggested that highly porous dust aggregates break through the radial drift barrier. In the minimum mass solar nebula model, highly porous icy dust aggregates can grow to planetesimal-size objects inside 10 AU (Okuzumi et al. 2012), though the model did not consider the evolution of the gas disk. It is necessary to take the gas disk evolution into account for the dust coagulation, because when the dust growth starts depends on physical conditions of the disk. In this study, we consider that both the evolution of the gas disk and the growth of the dust aggregates take place simultaneously. We simulate the viscous evolution of the gas disk starting from the molecular cloud core collapse and simulate the size evolution of icy dust aggregates with their porosities. As a result, we found that when the initial angular velocity of the molecular cloud core is large and the viscosity of the gas disk is small, dust aggregates can grow to planetesimal-size objects via direct collisional growth. In those cases, a large amount of icy dust particles can be supplied outside the snowline before icy aggregates start to drift toward the central star. Our results also suggest that icy planetesimals may be formed within a few hundred thousand years after starting the molecular cloud core collapse.

Orbital evolution of planetesimals in circumplanetary gas disks

*Hiroshi Kawamura¹, Keiji Ohtsuki¹, Ryo Suetsugu¹

1.Kobe University

Growing giant planets have circumplanetary disks around them in the late stage of their formation if their mass is sufficiently large. Regular satellites of the giant planets are orbiting in the prograde direction in approximately circular and co-planar orbits, thus they are thought to be formed in the circumplanetary disks. Clarification of the formation processes of regular satellites, which account for most of the total mass of the satellite system is essentially important. Shimizu & Ohtsuki (in preparation) investigated orbital evolution of planetesimals in circumplanetary gas disks by three body orbital integration neglecting gravitational interaction between planetesimals. Interaction between planetesimals may become important when they are large enough and are captured in mean motion resonances of the protosatellite. In the present work, we examine orbital evolution of planetesimals in circumplanetary gas disks by N-body simulation, taking account of their gravitational interaction.

Keywords: Satellite formation

Streaming instability in the dust layer of a protoplanetary disk

*ryo hasegawa¹

1.graduate school of science the university of tokyo

Two conflicting models are proposed to explain the process that dust grains grow to become planetesimals in the protoplanetary disk. One of them is that km-sized planetesimals are formed by the self-gravitational instability in a dust layer due to dust precipitation to the midplane. The gravitational instability occurs when the dust density exceeds a critical value. However, dust layer is believed to be in turbulent state, the layer would be dissipated. The streaming instability (Johansen & Youdin 2007) due to velocity shear between gas and dusts in the radial direction in the dust settling layer is a candidate to overcome this issue since the dust density increases locally even in the turbulent state.

We study the streaming instability by using hybrid simulations, where gas and dusts are treated as fluid and particles, respectively, and the dust-to-gas mass ratio is set to be ~ 1 .

We show the time history of the maximum dust density due to the instability in the dust layer.

Sintering of icy dust aggregates by vertical diffusion in a protoplanetary disk

*Kiriko Kodama¹, Sin-iti Sirono¹

1. Graduate School of Environmental Studies, Nagoya University

A protoplanetary disk consists of gas and dust grains. Coagulation of dust grains is the first step of planetary formation. Therefore, it is important to know whether dust grains can grow or not. There are two types of dust grains. One is made of ice and the other of rock. In this study, we focus on icy dust grains. Icy dust aggregates are sintered when they are heated. Sintering is the material transfer phenomenon to decrease total surface area. When an icy dust aggregate is sintered, its neck connecting dust grains grows. Because collision between sintered dust aggregates results in bouncing, they can not grow. Therefore, sintering greatly affects planetary formation. In a protoplanetary disk, the heat source is visible light irradiation from the central star. Because the dust grains around at the equatorial plane blocks the irradiation, only dust grains around the surface of a protoplanetary disk can be heated. Therefore, if turbulence transports an icy dust aggregate to the surface having high temperature, sintering can proceed.

Using temperature profile at the midplane, timescale required for sintering was estimated by Sirono (2011, ApJ, 735, 131). However, this study did not take account of the vertical diffusion of icy dust aggregates. In this study, we calculate the vertical motion of dust aggregates to clarify the sintering timescale by vertical diffusion.

The vertical motion of dust aggregates is diffusion by turbulence and sedimentation by gravity of the central star. We calculated the positions of aggregates as a function of time. Because sintering strongly depends on temperature (Sirono, 2011, ApJ, 735, 131), sintering of icy dust aggregates can be assumed to quickly proceed at certain height from the midplane. By numerical simulation we calculated the ratio of sintered dust aggregates that experienced high temperature to total number of aggregates. From this ratio, the sintering timescale is determined.

Distribution of dust aggregates reaches a steady state after the sedimentation timescale. In the steady state condition, each aggregate moves up and down in a vertical direction of a protoplanetary disk, icy dust aggregates are sintered if they exceed the altitude of high temperature. The fraction of sintered dust aggregates increases with time. The result can be well fitted by $1 - \exp(-t/b)$, where t is time and b is the sintering timescale. It is found that the sintering timescale gets shorter as the altitude of high temperature decreases. The sintering timescale is determined by the diffusion timescale that depend solely on the strength of turbulence irrespective of aggregate size. The altitude of high temperature depends on size of aggregates. As dust aggregates grow, the altitude goes down. Therefore, if they sufficiently grow, sintering by vertical diffusion of turbulence can proceed. It is possible that sintering by vertical diffusion hinders the growth of the aggregates.

Keywords: protoplanetary disk, dust aggregates, sintering, turbulence, diffusion

Water Delivery to Terrestrial Planets by Pebble Accretion

*Takeru Yamamura¹, Shigeru Ida¹

1.Department of Earth and Planetary Sciences, Graduate School of Science and Engineering, Tokyo Institute of Technology

The Earth would contain water of 0.023wt%-1wt% on the surface(ocean) and in the interior. It is observationally suggested that early Mars and early Venus had water. In particular, the water fraction of the early Mars may be comparable to that of the current Earth. Based on this information, we have investigated the water fraction of the Earth, Mars, Venus, and Mercury delivered by pebble accretion which is actively discussed today, numerically calculating the growth and inward migration of icy pebbles.

It is suggested that the snow line once migrated down to ~ 0.7 AU. Then, the terrestrial embryo gained water components from capturing migrating icy pebbles from outer parts of the protoplanetary disk. Because icy components have been subtracted in the outer disk, the gas in the terrestrial planet region should have been 'dry'.

Using this model, Sato et al. (2016) calculated the amount of water delivered to the Earth by icy pebble accretion and showed that a relatively small disk, strong turbulence, late passage of the snow line at 1 AU are required to be consistent with the inferred water content of the current Earth. We have generalized their simulation to a system of multiple planets (Earth, Mars, Venus and Mercury). While we used the same model of migration and formation of dust grains as Sato et al. (2016), we included decrease in pebble mass flux due to accretion by each planet. We found that the final water fraction of individual planets is directly determined by total amount of solid materials remaining in the disk. As long as the snow line passage timing at the individual planetary orbits is the same for all the planets, the final water fraction of individual planets should be similar to one another, while the amount of the water fraction depends on disk size, strength of turbulence, the timing of the snow line passage.

Keywords: pebble, water, planet

Simulation of the early Martian climate with denser CO₂ atmosphere using a general circulation model

*Arihiro Kamada¹, Takeshi Kuroda¹, Yasumasa Kasaba¹, Naoki Terada¹

1. Graduate School of Science, Tohoku University

The traces due to obvious liquid flow, which are thought to be made ~3.8 billion years ago, have been found on the Martian surface. They are believed to be made by the flow of liquid H₂O, and the environment of the ancient Mars is thought to be warmer and wetter than today. Several modeling studies have been performed for the investigation of the possible warming processes, but a study using a Martian general circulation model (MGCM) assuming the pure CO₂ atmosphere and the solar radiation corresponding to the time (~75% of today) [Forget et al., 2013] could not reproduce the surface temperature of higher than the melting point of H₂O, ~250 K in maximum, with the surface pressure of between 0.1 and 7 bars.

We are starting to reproduce the ancient Martian environment, in which the liquid flow existed on surface, using the DRAMATIC MGCM [e.g., Kuroda et al., 2005]. As a first step, we simulated the possible climate on early Mars with the pure CO₂ atmosphere and the global average of surface pressure of between 0.1 and 5.1 bars. In our simulations, the intensity of solar radiation is set to be 75% as large as today, assuming the ancient (~3.8 billion years ago) Mars, as well as Forget et al. [2013]. The same obliquity and eccentricity as today and very weak radiative effects of dust (opacity of 0.01) are adopted. Note that our model does not consider the infrared radiative effects of CO₂ ice clouds as implemented in Forget et al. [2013].

In the results of the simulations with the mean surface pressure of lower than 1 bar, the global mean skin temperature is almost constant to be ~192K, which corresponds to the radiative equilibrium temperature. It means that CO₂ infrared radiation in the 15 micro meter band does not work well under such a low temperature. In the simulations with the surface pressure of above 1 bar, global mean skin temperature increases with pressure, along with the CO₂ sublimation temperature. The regions with the surface temperature of near the CO₂ sublimation point (200-210K) spread globally, and it is considered that the emission of latent heat in the condensation processes stabilizes the temperature. However, our simulations show lower mean surface temperature than Forget et al. [2013], maximum for ~30 K with the mean surface pressure of 2-3 bars. The distance of temperature between the models becomes smaller with higher surface pressure, and become almost zero with 5 bars. One of the possible reasons is the radiative cooling of CO₂ ice clouds. In our simulation, column density of CO₂ ice clouds increases with the mean surface pressure of up to ~3 bars, so the absorption of long-wave radiation by the CO₂ ice clouds would possibly be critical. The other is the setting of albedo in the models. Between Forget et al. [2013] and our GCM the albedo of CO₂ ice sheet is different (0.5 and 0.65 correspondingly), which results in the lower surface temperature in our model with the mean surface pressure of 2-3 bars in which the area of CO₂ ice cloud spreads.

Keywords: Mars, Paleoclimate, General circulation model

Erosion and Replenishment of Atmosphere and Ocean on Earth during Heavy Bombardment

*Yui Kozasa¹, Hidenori Genda², Hiroyuki Kurokawa², Shigeru Ida^{1,2}

1.Department of Earth and Planetary Sciences, Tokyo Institute of Technology, 2.Earth-Life Science Institute, Tokyo Institute of Technology

After the Earth's formation, Earth experienced a lot of collisions of small objects such as asteroids and comets. These impacts, the so-called heavy bombardment, should have a great influence on the Earth's atmosphere. For example, the atmosphere can be eroded by the impact and also can be replenished by the volatile in the asteroid bodies. At the same time, Earth's ocean might exist in the early stage (Wilde et al., 2001). Therefore the ocean would also experience the erosion and replenishment by these impacts. The purpose of this work is to investigate the effects of these impacts on atmosphere and ocean throughout this heavy bombardment event.

There are several previous papers on atmospheric erosion caused by just one impact (Svetsov 2000, 2007; Shuvalov 2009, 2014). In these papers, the eroded atmosphere mass by a single impact was analytically and/or numerically investigated, and its dependence to impact parameters (e.g. impactor diameter, impact velocity, atmosphere pressure,) is formulated as the equations with several parameter sets. For a long-term evolution, de Niem et al. (2012) focused on the atmosphere erosion and replenishment during LHB (late heavy bombardment), which is thought to happen during 3.8 Ga. During LHB, the total impactor mass is less than 0.01% of Earth mass. By Monte Carlo approach, de Niem et al. (2012) found that the atmospheric pressure strongly increases both in Earth and Mars during LHB.

In our study, we also use a Monte Carlo calculation of atmosphere and ocean simultaneously. To consider the whole term of heavy bombardment, we computed until the total impactor mass reaches 1% of the Earth mass. We also used several atmospheric erosion models to study how the mass change behavior depends on the model. To regard the ocean mass evolution, the erosion mass of ocean is taken from the target loss mass in Svetsov (2009), which was calculated simultaneously with the atmospheric erosion. We applied the water density as the target density. For Monte Carlo calculation, we used the current size distribution of the Main belt asteroids. Impact velocity distribution is taken from a numerical model, and we used three parameters for the volatile and water content of asteroids.

As a result, the atmosphere is extensively eroded in the model of Svetsov (2000, 2007), and the atmospheric pressure converges to a certain value, which depends on the concentration of volatile amount in impactors, regardless of the pre-existing atmospheric pressure. However, the erosion of the atmosphere is minor in the model of Shuvalov (2014). The behavior of the atmospheric mass strongly depends on the erosion models used in the computation. The ocean erosion did not depend on the atmosphere in spite of the impact energy dependency to atmosphere pressure in Svetsov (2009). The erosion of the ocean is moderate than that of atmosphere. Therefore, the final ocean depth depend on the pre-existing ocean mass and water content of the impactor.

From the results of Svetsov (2000, 2007) model, the combination of extensive erosion of atmosphere and moderate erosion of ocean would explain the difference of H/C ratio between carbonaceous chondrites and the Earth's hydrosphere or bulk silicate Earth (Hirschmann & Dasgupta 2009). Also, the erosion of pre-existing atmosphere is considerable. It depends on the parameter, but the remaining ratio would be only 0.0001-10%. For this, the heavy bombardment can erode massive H-He protoatmosphere, even if the Earth got the surrounding nebular gas (Ikoma & Genda 2006). The erosion of pre-existing ocean might explain the problem that the Earth is depleted in halogen elements such as Cl, Br, and I (Sharp & Draper 2013), by thinking the elements being dissolved into

pre-existing ocean. However, in this study the ocean erosion was not effective. The erosion of pre-existing ocean is estimated about 20%, and it is not enough to explain the whole depletion of Halogen.

Keywords: heavy bombardment, atmospheric erosion, oceanic erosion

The evolutionary climatic track of the hypothetical Earth with different conditions of central star and semi-major axis

*Shintaro Kadoya¹, Eiichi Tajika²

1.Department of Earth and Planetary Science, The University of Tokyo, 2.Department of Complexity Science and Engineering, The University of Tokyo

The climate of the Earth is affected strongly by the insolation from the Sun and also by the amount of greenhouse gasses, especially CO₂, in the atmosphere. The former depends on the mass and age of the central star, and the semi-major axis of the planet, while the latter depends on the degassing rate of CO₂, which, in turn, depends on the thermal evolution of the planetary interiors. Thus, the climate of the Earth may be controlled both by the evolution of the planetary interior and the evolution of the host star. It is however unknown how the climate of planet could evolve if the central star and semi-major axes are different from those of the Earth today. In this study, we examine the climatic evolution of the Earth with different conditions of host stars and orbital semi-major axes.

We use a one-dimensional energy balance model coupled with a carbon cycle model to estimate the climate, a parameterized convection model coupled with a mantle degassing model to estimate the evolution of the CO₂ degassing rate, and a standard evolution model of the Sun with a relationship between mass and lifetime of main sequence stars to estimate the evolution of luminosity of the central star.

We found that, while the climate of the Earth orbiting at the inner region of the habitable zone (HZ) becomes hot owing to the increase in the luminosity of the central star, the climate of the Earth orbiting at the outer region of the HZ becomes cold because the CO₂ degassing rate of the Earth decreases with time. In particular, the Earth orbiting at the outer region of the HZ becomes the snowball climate mode after 3 Gyr, irrespective of the mass of the central star. This timescale depends mainly on the planetary parameters, such as the land fraction and land distribution. Thus, the lifetime of the habitability of the planets orbiting at the outer region of HZ is controlled largely by the evolution of the planetary interiors rather than the stellar evolution. This is essentially because the greenhouse effect of CO₂ is necessary for the planets orbiting even in the HZ to have a warm and wet climate.

Keywords: Carbonate-silicate geochemical cycle